Ionization of Clusters in Intense Laser Pulses through Collective Electron Dynamics

Ulf Saalmann and Jan-Michael Rost

Max-Planck-Institut für Physik komplexer Systeme, Nöthnitzer Straße 38, 01187 Dresden, Germany

The motion of electrons and ions in medium-sized rare gas clusters (~1000 atoms) exposed to intense laser pulses is studied microscopically by means of classical molecular dynamics using a hierarchical tree code. Pulse parameters for optimum ionization are found to be wavelength dependent. This resonant behavior is traced back to a collective electron oscillation inside the charged cluster. It is shown that this dynamics can be well described by a driven and damped harmonic oscillator allowing for a clear discrimination against other energy absorption mechanisms.

     PACS numbers: 36.40.Gk, 31.15.Qg, 36.40.Wa

The interaction of intense laser radiation with clusters has been of continuing interest [1–7], pushed by prominent findings as the emission of keV photons [1], highly charged ions [2,3], or fast fragments [4]. Basically, all these phenomena are caused by the exceedingly effective absorption of energy from the laser field into the cluster. This enhanced absorption (when compared to atoms or bulk matter) is possible due to the initially *solidlike atomic density in the cluster* in combination with the *rapid expansion of the cluster* on a femtosecond time scale, i.e., typically during the laser pulse. More detailed insight into the mechanism of energy absorption can be gained by pulse length variation. Using pulses of equal energy, i.e., longer pulses have lower intensities, it has been found that there is an optimum pulse length with maximum absorption [5,6]. This holds true for small rare gas and metal clusters (of the order of some 10 atoms) as well as for large clusters, although the underlying reason for maximum absorption can be very different and is, in fact, an issue of current debate. For small rare gas clusters under laser pulses of peak intensities in the tunneling regime ($I \gtrsim 10^{15}$ W/cm^2) such an optimum could be attributed to the mechanism of enhanced ionization [8] known from molecules [9]. For small metal clusters exposed to similar laser pulses the existence of optimal absorption was interpreted as a plasmon resonance phenomenon [6] in analogy to the well known dipole resonance of the valence electrons in perturbative photoabsorption [10] or low-intensity laser pulses [11]. For large clusters (of more than 10^5 atoms) it has been proposed that strong laser pulses create a nanoplasma inside the cluster [12,13]. In the course of the expansion of the cluster the electron density and consequently the plasma frequency decreases, resulting in strong energy absorption at resonance with the laser.

Separating the different mechanisms from each other requires specific and clear signatures for each process which are difficult to identify in a multiparticle system such as a cluster. Surprisingly, dipole resonant absorption dynamics in a cluster can be very well characterized by a simple driven damped harmonic oscillator, which de-scribes the dipole response of the electrons inside the cluster.

In the following we will demonstrate the validity of this simple description with full dynamical microscopic calculations for xenon clusters (~$10^2 \ldots 10^3$ atoms) in strong optical laser pulses (wavelengths $\lambda = 520 \ldots 1170$ nm, intensities $I \sim 10^{14} \ldots 10^{16}$ W/cm^2, pulse lengths $T \sim 10 \ldots 1000$ fs). Our approach is similar to those used before for intense laser-cluster interaction [14]. However, we have been forced to use a completely new propagation scheme, namely, a hierarchical tree code [15], to handle of the order of 10^4 charged particles (~1000 ions and ~8000 electrons) with their mutual interactions. Originally developed for gravitational N-body problems in cosmology [16], the hierarchical tree code allows us to follow the dynamics of all charged particles over a few hundred femtoseconds with typical time steps of attoseconds.

Atoms are initially arranged in so-called Mackay icosahedra [17] known to be optimal structures of Lennard-Jones clusters. We distinguish between free and bound electrons, whereby the latter ones are not treated explicitly. The condition for creation of an electron is that none of the other electrons has a negative binding energy to the ion under consideration. In this case a new electron is "born" at the position of that ion with a kinetic energy to satisfy the ionization potential. The charge of the ion is increased by one. Free electrons as well as ions are described classically as charged particles in an oscillating field interacting via a softened Coulomb interaction W. This is defined for a pair of particles with charges q_1 and q_2 and a distance of r_{12} as $W = q_1 q_2 / \sqrt{r_{12}^2 + 1}$.

First of all, we present the calculated pulse length dependence for three different laser wavelengths λ. Figure 1 shows the final averaged charge state per atom from Xe$_{561}$ clusters after laser impact as a function of the pulse length T or the peak intensity I, respectively. Another observable in experiments is the maximal kinetic energy of the exploding ions [2]. It shows a similar dependence on the pulse length [18] as the charge in Fig. 1.
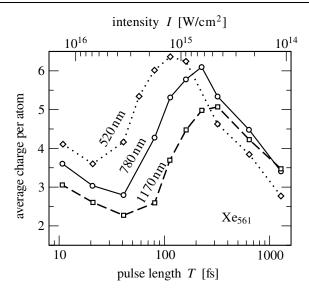
FIG. 1. Average charge per atom from Xe_{561} clusters after laser impact according to Eq. (1) as a function of the pulse length T or the peak intensity I, respectively, for three different laser wavelengths λ. The energy of the pulse, i.e., the product $I \times T$, is kept constant.

The applied laser pulse was linearly polarized with a field

$$F(t) = \begin{cases} \sqrt{I/I_0}\cos^2(\frac{\pi t}{2T}) \cos(\omega t), & \text{for } |t| < T, \\ 0, & \text{elsewhere,} \end{cases} \quad (1)$$

where $I_0 = 3.51 \times 10^{16} \text{ W/cm}^2$. In order to keep the energy of the different pulses constant we fixed the product of intensity and pulse length $I \times T = I_0 \times 4$ fs. For short pulses ($T \lesssim 30$ fs), where the cluster atoms have not enough time to react on the charging, the final charge state decreases with an increasing pulse length due to the lower intensity. For longer pulses ($T \gtrsim 50$ fs), however, the final charge state increases despite the intensities becoming smaller. This can be understood only if one considers the expansion of the cluster; for a detailed explanation see below. Finally, for very long pulses ($T \gtrsim 400$ fs) the cluster is already completely fragmented before the laser pulse reaches its peak intensity rendering the ionization similar compared to the case of single atoms. Qualitatively, this behavior is the same for all three frequencies (Fig. 1). However, the shift of the optimal pulse length towards longer pulses for longer wavelengths is characteristic for a resonant ionization mechanism. A corresponding shift of the optimum has been obtained for the maximal kinetic energy of the exploding ions [18].

To gain insight into the mechanism of ionization we discuss the dynamics of a Xe_{923} cluster in a laser pulse with $I = 9 \times 10^{14} \text{ W/cm}^2$; cf. Fig. 2. The pulse has short rise and fall times of 20 fs and a long plateau of 160 fs in order to eliminate effects from the time dependence of the laser pulse itself. As can be clearly seen in Fig. 2(a), the cluster ionization occurs in two steps, and the total
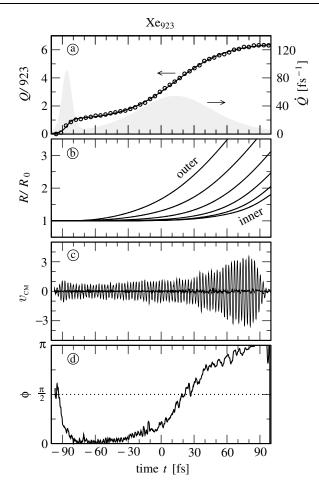

FIG. 2. Dynamics of Xe_{923} in a strong laser pulse ($\lambda = 780$ nm, $I = 9 \times 10^{14} \text{ W/cm}^2$, rise and fall time 20 fs, plateau for $t = -80 \ldots + 80$ fs). All quantities are shown as a function of time t. (a) Average charge per atom (circles and fit from Eq. (2), left axis) and corresponding rate (gray filled line, right axis). (b) Radii R of all cluster shells in units of their initial radii R_0. (c) Center-of-mass velocity v_{CM} of the electronic cloud inside the cluster volume. Note that the oscillations are spatially along the linear polarization of the laser, whereas the electron velocity perpendicular to the laser polarization is very small and hard to see in the figure. (d) Phase shift ϕ_t of the collective oscillation in the laser direction with respect to the driving laser; see text.

cluster charge Q (sum of total ionic charge Q_{ion} and charge of those electrons which are inside the cluster volume) as a function of time t is well represented by

$$Q(t) = \sum_{i=1,2} \frac{Q_i}{1 + \exp(-(t - t_i)/\delta t_i)}. \quad (2)$$

In the first step during the rising of the pulse ($t_1 \pm \delta t_1 = -86 \pm 3$ fs) electrons are emitted mainly due to field ionization. This process slows down, however, already before the plateau intensity is reached due to the increasing space charge (cluster charge $Q \approx 1000$ at $t = -80$ fs). Because of this attractive space charge, one may distinguish between inner ionization, which accounts for excitation

from localized electrons to quasifree electrons moving inside the cluster volume, and outer ionization, which corresponds to the final escape of the quasifree electrons from the cluster into the continuum. Note that the space charge can hold an appreciable number of quasifree electrons which engage in the collective motion discussed below, in contrast to the ionization dynamics of molecules or small clusters with almost no quasifree electrons [8]. The charging up of the cluster leads to an expansion as can be seen for $t \gtrsim -60$ fs in Fig. 2(b). During the expansion a second ionization step occurs which lasts for a much longer time and leads to an increase of the average ionic charge from about 1 to more than 6. During this time, the quasifree electrons in the cluster are driven collectively back and forth along the polarization direction of the laser which is evident from their center-of-mass (CM) velocity v_{CM} shown in Fig. 2(c).

This oscillation can be modeled by a driven and damped classical harmonic oscillator

$$\ddot{X}(t) + 2\Gamma_t \dot{X}(t) + \Omega_t^2 X(t) = F(t) \quad (3)$$

with $X(t)$ the CM position of the electron cloud, $F(t)$ the driving laser amplitude, and Ω_t and Γ_t the eigenfrequency and damping rate, respectively, which are determined by the cluster. The index t indicates that due to ionization and expansion of the cluster, both Ω_t and Γ_t may depend parametrically on time. Under the assumption of a spherical, uniformly charged cluster with total ionic charge Q_{ion} and radius R the potential inside the cluster is harmonic with an eigenfrequency $\Omega_t = \sqrt{Q_{ion}(t)/R(t)^3}$. The damping is caused by both internal heating of the quasifree electrons in the cloud and energy transfer to bound electrons. These two effects are responsible for outer and inner ionization, respectively.

For periodic driving $F(t) = F_0 \cos(\omega t)$ the dynamics is given by $X(t) = A_t \cos(\omega t - \phi_t)$ with [19]

$$A_t = F_0/\sqrt{(\Omega_t^2 - \omega^2)^2 + (2\Gamma_t \omega)^2}, \quad (4a)$$

$$\phi_t = \arctan[2\Gamma_t \omega/(\Omega_t^2 - \omega^2)]. \quad (4b)$$

The energy balance of the dynamics (4) is characterized, on one hand, by energy loss E_{loss} due to the damping and, on the other hand, by energy gain E_{gain} from the external laser field. The cycle-averaged energy transfer rates read

$$\langle \dot{E} \rangle = \langle \dot{E}_{loss} \rangle + \langle \dot{E}_{gain} \rangle = -\Gamma_t A_t^2 \omega^2 + \tfrac{1}{2} F_0 A_t \omega \sin\phi_t. \quad (5)$$

Obviously and well known [19], maximum $\langle \dot{E}_{gain} \rangle$ or optimal heating requires $\phi_t = \pi/2$, i.e., resonant behavior $\Omega_t = \omega$. As shown in Fig. 2(d), the phase shift ϕ_t changes in time from 0 to π, thereby passing the resonance $\phi_t = \pi/2$. This change is directly connected with the increased ionization of the cluster; cf. Fig. 2(a). In particular, the resonance time t_{res} coincides with the time t_2 of maximal ionization rate; cf. Eq. (2). This

applies to other laser wavelengths as well (for $\lambda = 1170$ nm, t_2 is somewhat smaller due to the early laser switch off at $t = 80$ fs):

λ_{laser}	520 nm	780 nm	1170 nm
$t_2 \pm \delta t_2$	(-24 ± 13) fs	(13 ± 24) fs	(40 ± 26) fs
t_{res}	-22 fs	19 fs	72 fs

Passing through the resonance is not necessarily connected with large amplitude oscillations, if the damping strength Γ_t is comparable to or larger than the eigenfrequency Ω_t; see Fig. 3. Otherwise, the phase shift ϕ_t at resonance is independent of the damping (Fig. 3).

In order to validate the applicability of the driven and damped harmonic oscillator model of Eq. (3) we use amplitude A_t and phase shift ϕ_t of the collective oscillation from our results of Fig. 2 to determine frequency and damping rate according to

$$\Omega_t^2 = \omega^2 + (F_0/A_t)\cos\phi_t, \quad (6a)$$

$$\Gamma_t = [F_0/(2A_t\omega)]\sin\phi_t. \quad (6b)$$

Figure 4 shows these parameters as a function of time t for the same system as in Fig. 2. The calculated eigenfrequency Ω_t (gray circles in Fig. 4) closely resembles the frequency of a uniformly charged sphere (solid line). Moreover, both frequencies match the laser frequency ω at the same time $t \approx 20$ fs providing additional support for the collective oscillator model. Along with the decrease of the eigenfrequency Ω_t the damping term Γ_t (white diamonds in Fig. 4) rises for times $t \approx -60 \dots 30$ fs. This accounts for energy transfer to deeper and deeper bound electrons, which does not occur in other theoretical studies where also resonant behavior was discussed [20,21]. Either inner ionization was not considered [20] or deuterium clusters composed of single electron atoms were discussed [21]. However, in order to understand the experimentally observed high charge states [2,3,5,6] it is of utmost importance to take this into consideration. It is just this continuous cycle of effective
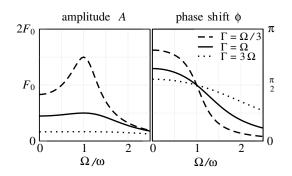

FIG. 3. Driven and damped harmonic oscillator: amplitude A and phase shift ϕ as a function of the ratio of eigenfrequency Ω and driving frequency ω according to Eqs. (4) for different damping strengths Γ.
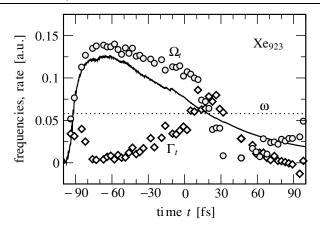
FIG. 4.   Parameters of the harmonic oscillator model (3) as calculated from the Xe_{923} dynamics in Fig. 2. Solid line: eigenfrequency for a spherical, uniformly charged cluster $\Omega_t = \sqrt{Q_{ion}(t)/R(t)^3}$. Circles: eigenfrequency Ω_t (6a). Diamonds: damping rate Γ_t (6b). Dotted line: laser frequency ω.

heating and induced inner ionization at the resonance which causes the increased ionization rate and the high charge states of the fragments. At this point it is interesting to note that the damping almost completely compensates the heating as can be deduced from the almost negligible increase of the amplitude of v_{CM} before reaching the resonance [Fig. 2(c)]. Once the cluster has passed the resonance, however, the damping falls off rapidly ($t \gtrsim 30$ fs in Fig. 4). Obviously, the oscillating electron cloud becomes unable to drive further inner ionization. This implies a weaker damping and thus an increase of the oscillation amplitude; cf. Fig. 2(c).

In summary, we have shown that the electron emission in medium-sized rare gas clusters ($\sim 10^3$ atoms) is enhanced by resonant energy absorption in agreement with experimental data [5,6]. (The metallic nature of the clusters used in [6] should be of minor importance for the creation of the high charge states $\gtrsim 8$ since the delocalized valence electrons are emitted early in the pulse.) Our microscopic calculations of the motion of ions and electrons using a hierarchical tree code reveal a laser-driven collective oscillation of the cloud of quasifree electrons which are held back inside the cluster volume by the space charge of the cluster. The eigenfrequency of this oscillation is determined by charge and size of the cluster. Electron emission and cluster expansion change these quantities in time and eventually enable the matching of eigenfrequency Ω_t and laser frequency ω during the pulse. This resonance allows for an effective energy transfer to the collective motion. The changing phase shift between driving field and driven electron cloud clearly indicates the different stages of energy absorption of the cluster electrons from the laser field. The fact that the collective electron dynamics can be well described by a simple damped harmonic oscillator helps to clarify the

nature of this dynamics and provides a clear signature of this type of collective dynamics. We expect that the other two mechanisms for effective energy absorption, namely, enhanced ionization and nanoplasma excitation will have an almost vanishing amplitude for the electronic CM velocity. Small clusters, which exhibit enhanced ionization, produce only a few quasifree electrons which cannot create a sizable CM-velocity amplitude. In large clusters, however, where a nanoplasma is formed, electrons are heated resonantly at their critical density leaving their CM position at rest.

[1] A. McPherson, B. D. Thompson, A. B. Borisov, K. Boyer, and C. K. Rhodes, Nature (London) **370**, 631 (1994).
[2] T. Ditmire, J. W. G. Tisch, E. Springate, M. B. Mason, N. Hay, R. A. Smith, J. Marangos, and M. H. R. Hutchinson, Nature (London) **386**, 54 (1997).
[3] M. Lezius, S. Dobosz, D. Normand, and M. Schmidt, Phys. Rev. Lett. **80**, 261 (1998).
[4] T. Ditmire, J. Zweiback, V. P. Yanovsky, T. E. Cowan, G. Hays, and K. B. Wharton, Nature (London) **398**, 489 (1999).
[5] J. Zweiback, T. Ditmire, and M. D. Perry, Phys. Rev. A **59**, R3166 (1999).
[6] L. Köller, M. Schumacher, J. Köhn, S. Teuber, J. Tiggesbäumker, and K. H. Meiwes-Broer, Phys. Rev. Lett. **82**, 3783 (1999).
[7] *Molecules and Clusters in Intense Laser Fields*, edited by J. Posthumus (Cambridge University Press, Cambridge, U.K., 2001).
[8] Ch. Siedschlag and J. M. Rost, Phys. Rev. Lett. **89**, 173401 (2002); Phys. Rev. A **67**, 013404 (2003).
[9] T. Zuo and A. D. Bandrauk, Phys. Rev. A **52**, R2511 (1995); T. Seideman, M. Yu. Ivanov, and P. B. Corkum, Phys. Rev. Lett. **75**, 2819 (1995).
[10] M. Brack, Rev. Mod. Phys. **65**, 677 (1993).
[11] E. Suraud and P. G. Reinhard, Phys. Rev. Lett. **85**, 2296 (2000).
[12] T. Ditmire, T. Donnelly, A. M. Rubenchik, R. W. Falcone, and M. D. Perry, Phys. Rev. A **53**, 3379 (1996).
[13] H. M. Milchberg, S. J. McNaught, and E. Parra, Phys. Rev. E **64**, 056402 (2001).
[14] C. Rose-Petruck, K. J. Schafer, K. R. Wilson, and C. P. J. Barty, Phys. Rev. A **55**, 1182 (1997).
[15] S. Pfalzner and P. Gibbon, *Many-Body Tree Methods in Physics* (Cambridge University Press, Cambridge, U.K., 1996).
[16] J. E. Barnes and P. Hut, Nature (London) **324**, 446 (1986).
[17] M. R. Hoare, Adv. Chem. Phys. **XL**, 49 (1979).
[18] U. Saalmann and J. M. Rost (unpublished).
[19] L. D. Landau and E. M. Lifschitz, *Mechanics* (Pergamon Press, Oxford, 1994).
[20] I. Last and J. Jortner, Phys. Rev. A **60**, 2215 (1999).
[21] P. B. Parks, T. E. Cowan, R. B. Stephens, and E. M. Campbell, Phys. Rev. A **63**, 063203 (2001).